

MASSACHUSETTS INSTITUTE OF TECHNOLOGY

3.014 Materials Laboratory
Fall 2005

LABORATORY 4: Module 7₃

Structural Changes in Alkali Borate Network Glasses

Instructor: Professor Linn W. Hobbs

Objectives

- Experience the glass transition through observing temperature dependence of viscosity
- Observe change in glass transition effected by changes in glass composition
- Relate thermal and spectroscopic features to glass network structure

Tasks

- Prepare sodium borate glass melts and draw sodium borate glass fibers
- Measure glass transition temperature with differential thermal analysis
- Deduce network entities from laser Raman spectroscopy

Materials

- Sodium carbonate powder (Na_2CO_3), 250g
- Boric acid powder (H_3BO_3), 500g
- 8 Alumina crucibles, 50ml
- 8 Silica glass rods, 4-mm diameter

Introduction

A *GLASS* is, formally, a solid that solidifies without a well-defined melting point—defined as a singular temperature at which there occurs a discontinuous change in a physical property, for example specific volume, during transition between a liquid state and its corresponding solid state—but instead exhibits a continuous change in that property over a range of temperature. Glasses tend to inherit their atomic-scale structures from those of the liquids from which they evolve by cooling, and their structural arrangements are therefore necessarily less-ordered than those of corresponding crystalline arrangements. Such glassy arrangements are often termed *amorphous*, though formally again what is meant by this term is lack of the long-range translational and rotational regularity that characterize crystalline arrangements. All “amorphous” atom arrangements do not necessarily exhibit a formal *glass transition*, though many do. Good examples are 1) vitreous silica [SiO_2] (also known as “fused quartz” because in its production crystalline quartz is melted, then cooled rapidly enough to ensure that

crystallization does not take place); 2) soda-lime glass (“window glass”) formed by dissolving sodium and calcium oxides into a silica melt and cooling; 3) aluminoborosilicate labware glasses like Pyrex.[®]

Chemical bonding of atoms—whether ionic, covalent or metallic in character—governs the coordination of other atoms around any given atom in a solid. For metallic and ionic solids, atom or ion sizes are a principal factor in determining coordination, which tends to be high (usually between 6 and 12). The orbital geometries and directivity of covalent bonds occasion rather lower coordination (typically 2 to 4). The preferred coordination is clearly critical in deciding the crystal structure adopted in crystalline solids. The coordination established by chemical bonding in less regular atomic arrangements—for example, glasses—is often similar or identical to that in crystals and is equally important in deciding the structure of non-crystalline solids. The connectivity of coordinated groups of atoms in turn governs many mechanical responses of the non-crystalline solid. This experiment explores the consequences—for the propagation of mechanical vibrations—of changes in the nature of the network bonding and structure in alkali borate glasses.

Lacking the “crutch of periodicity” that enables even complicated inorganic crystal structures to be described by a few, or a few tens of, atoms in a uniform unit cell, glass structures resist description and are still partly a matter for speculation. One useful approach, first addressed by the noted American crystal chemist William H. Zachariasen in 1932 in the only paper he published on glass structure,¹ starts with connectivity—which atoms are likely to be connected to which other atoms—and seeks empirically to construct a network that resists shear (thus distinguishing it from a liquid), lacks long-range translational and orientational regularity (thus distinguishing it from a crystalline arrangement), and can be extended indefinitely. Zachariasen chose as his paradigm vitreous silica, a three-dimensional oxide network glass, in which silicon atoms are invariably surrounded by four oxygen atoms, forming $[\text{SiO}_4]$ tetrahedral units that connect to each other by sharing common oxygen atoms at each of their four vertices. But in the simpler heuristic depiction he chose to illustrate, Zachariasen used $[\text{AO}_3]$ equilateral triangular units, sharing each of their three vertex oxygens with other triangular units in two dimensions.

It is, of course, trivial to extend a network of corner-sharing triangles indefinitely in two dimensions if the triangles are oriented identically to form a hexagonal crystalline network. But Zachariasen found that he could extend such a network seemingly indefinitely even if the triangles were *randomly* rotated with respect to each other (random A-O-A angle). His model, later coined the “continuous random network” by MIT X-ray crystallographer and physics professor Bertram E. Warren² (MIT SB ’24, SM ’25, DSc ’29) who studied glass structure by X-ray diffraction in the 1950’s, has become the standard textbook illustration for network glass structure (even though the model was not proven extendable to three dimensions until the 1990’s).

¹W. H. Zachariasen, *J. Amer. Chem. Soc.* **54** (1932) 3841-3851.

²B. E. Warren, *J. Amer. Ceram. Soc.* **17** (1934) 249.

Topology and Rigidity

A more rigorous approach to description of glass structure employs the mathematics of network topology³ (much explored in the last two decades because of the importance of pervasive computer networks) and analyzes continuous closed paths, called *rings*, in a network of connected *polytopes* (geometrical coordination units, like the [SiO₄] tetrahedra or [AO₃] triangles of the last two examples). Moreover, a topological approach can explain why solids form non-crystalline structures at all. The reason is related to rigidity theory⁴, a formal exploration of which was first undertaken by James Clerk Maxwell⁵, the mid-19th century Cambridge University physicist whose compact formulation of the laws governing electromagnetic phenomena are now known as Maxwell's relations. Maxwell discovered that rigid connected structures, like a bridge truss, derive their stability from the fact that the degrees of freedom at the connection points of the structure (3 degrees of freedom in three-dimensions) are exceeded by the constraints imposed on that freedom by the connections to other parts of the structure. Ceramists Alfred R. Cooper (MIT Ph.D. '60 and former Course III professor) and his former student Prabat K. Gupta (now a professor at Ohio State University) codified these constraints for arbitrary polytopes (rods, triangles, tetrahedral, octahedral, cubes...) and connectivity motifs (vertex-sharing, edge-sharing, face-sharing) and established a parameter called *structural freedom f* to describe the excess of freedoms over constraints, which was found to correlate with glass-forming ability⁶ and amorphizability⁴. Their analysis yields

$$f = d - C\{\delta - [\delta(\delta+1)/2V]\} - (d-1)(Y/2) - [(p-1)d - (2p-3)](Z/p) \quad (1)$$

where d is dimension of the structure (1-, 2- or 3-dimensional), δ is the dimension of the polytope, C (the "connectivity") is the number of polytopes with V vertices meeting at a vertex, Y is the fraction of vertices which participate in sharing of edges (defined by 2 adjacent vertices), and Z is the fraction of vertices that participate in sharing of p -sided faces. As an instructive example, MgO (with the rocksalt structure) is comprised of [MgO₆] octahedra sharing each of their six edges with five other adjacent octahedra ; the parameters

³L. W. Hobbs, C. E. Jesurum, V. Pulim and B. Berger, "Local topology of silica networks," *Philos. Mag.* **A 78** (1998) 679-711. L. W. Hobbs, C. Esther Jesurum and Bonnie Berger, "The topology of silica networks," Chapter 1 in: *Structure and Imperfections in Amorphous and Crystalline Silica*, ed. J.-P. Duraud, R. A. B. Devine and E. Dooryhee (John Wiley & Sons, London, 2000) pp. 1-47. Linn W. Hobbs and Xianglong Yuan, "Topology and Topological Disorder in Silica," in: *Defects in SiO₂ and Related Dielectrics: Science and Technology*, ed. G. Pacchioni, L. Skuja and D. L. Griscom (Kluwer, Dordrecht, Netherlands, 2000) pp. 37-71.

⁴Linn W. Hobbs, C. Esther Jesurum and Bonnie Berger, "Rigidity constraints in the amorphization of singly- and multiply-polytopic structures," in: *Rigidity Theory and Applications*, ed. P. M. Duxbury and M. F. Thorpe (Plenum Press, New York, 1999) 191-216.

⁵J. C. Maxwell, *Philos. Mag.* **27** (1864) 294.

⁶P. K. Gupta and A. R. Cooper, *J. Non-Crystalline Solids* **123** (1990) 14. P. K. Gupta, *J. Amer. Ceram. Soc.* **76** (1993) 1088.

for (1) are ($d = 3, \delta = 3, V = 6, C = 6, Y = 1, Z = 0$) and yield $f = -10$. The large negative value of f means that MgO is extraordinarily *overconstrained* and proves virtually impossible to amorphize: it always solidifies or self-assembles into the crystalline state and will retain that structure without rearrangement even when a large fraction of the interionic connections are missing. By contrast, SiO₂ comprises [SiO₄] tetrahedra sharing each of their four vertices with another tetrahedron ($d = 3, \delta = 3, V = 4, C = 2, Y = 0, Z = 0$) and yields $f = 0$. SiO₂ structures are therefore only marginally constrained, and breaking only a small number of bonds renders the structure floppy and able to rearrange and rebond into many alternative arrangements, most of them non-crystalline, with only small differences in internal energy from those of crystalline silica structures. Silica, with $f = 0$, is the archetypal glass former.

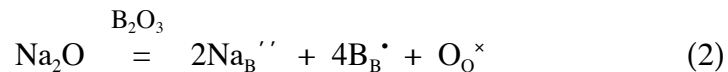
Borate Glasses

SiO₂ forms [SiO₄] tetrahedra because the single filled 3s and two half-filled 3p Si orbitals (containing a total of 4 electrons) hybridize to form four “sp₃ bonds,” each containing a single unpaired electron, pointing to the corners of a tetrahedron at mutual angles of about 107°. [The silicon atom (atomic number $Z = 14$) electronic structure is: $1s^2 2s^2 2p^6 3s^2 3p_x^1 3p_y^1$.] Each of the four “sp₃ bonds” reaches out to one of the two half-filled oxygen 2p orbitals in a neighboring oxygen atom, each containing a single electron [oxygen ($Z = 8$) electronic structure: $1s^2 2s^2 2p_z^2 2p_x^1 2p_y^1$] to form an Si-O “bond” containing a pair of electrons. Thus, each Si is tetrahedrally coordinated by four O atoms (in [SiO₄] tetrahedral polytopes) and each O (the other half-filled O 2p orbital reaching out to a second Si) is coordinated by two Si atoms, with an Si-O-Si angle that can take on values between about 120° and 180°. Carbon ($Z = 6$, electronic structure: $1s^2 2s^2 2p_x^1 2p_y^1$) analogously hybridizes the single filled 2s and two half-filled 2p orbitals to form the strong tetrahedral “sp₃” bonds in diamond; but it can also hybridize the 2s² orbital electrons with a single electron from one 2p orbital to form three “sp₂” bonds at 120° holding together the planar hexagonal layers of graphite, the remaining 2p_z orbital electron available to effect weaker interlayer bonding.

Boron (atomic number $Z = 5$, electronic structure: $1s^2 2s^2 2p_x^1$) can perform the same trick. Hybridization of the filled 2s and half-filled single 2p_x orbital yields three “sp₂” bonds at 120°, so that boron combines with oxygen as [BO₃] triangular polytopes which share corner oxygens to form two-dimensional network sheets with composition B₂O₃ (with *no* O 2p orbital electron left over to effect bonding between sheets, as in graphite). This structure is exactly the two-dimensional Zachariasen model, for which $d = 2, \delta = 2, V = 3, C = 2$ and $f = 0$. In three dimensions, $d = 3$, and structural freedom for B₂O₃ is increased to $f = +1$; thus, in the three-dimensional solid, a certain floppiness of the network is expected, or at least it is not expected to exhibit a high stiffness. As expected, B₂O₃ is a facile glass former and is, in fact, difficult to retain in crystalline form. There is evidence that about 70% of the [BO₃] triangles arrange themselves into [B₃O₆] super-structural units called *boroxyl rings*, each boroxyl unit comprising three triangles in a 3-ring. The superstructure units are connected to other [BO₃] triangles or other boroxyl rings through three common oxygens per unit, just as are [BO₃] triangles, so the boroxyl units are just larger triangular polytopes, and the fundamental topology is not changed.

Because glasses undergoing a glass transition change continuously from a liquid (of low viscosity) to a solid (of effectively infinite viscosity) when cooled, the point of “solidification” is defined operationally as when the viscosity reaches a critical value (taken as 10^{13} Pa s) at a temperature called the glass transition temperature (T_g). If an alkali (or alkaline earth) oxide, like Na_2O is added to SiO_2 , it has been known for at least four millennia that the viscosity of silica glass is substantially reduced, so that it can be poured or worked (viscosities of 10^3 - 10^7 Pa s) at temperatures as low as 700°C , easily accessible to ancient pyrotechnologies. This phenomenon is the basis of the soda-lime silicate glass compositions (16mol% Na_2O -10mol% CaO -74mol% SiO_2) still in common use today—for beer bottles and window glass, for example. The explanation is that the large, highly ionic alkali or alkaline earth ions prefer to be coordinated by as many oxygen atoms as possible; this coordination can only be achieved if network Si-O bonds are broken, leaving some oxygens connected to the network through only one, not two bonds (these are called “non-bridging oxygens,” or NBOs), each NBO being left with an electron in a “dangling” 2p orbital that can interact strongly with positively charged alkali ions, which then distribute themselves in regions of locally high NBO density. In fact, Na_2O is readily soluble in SiO_2 because Na ion goes from 4-fold coordination by oxygen in the anti-fluorite structure of Na_2O to higher average oxygen coordination in the sodium silicate glass. The resulting structure is called a “modified random network” and is less connected, exhibiting lowered viscosity and stiffness at a given temperature and a reduction of T_g from $\sim 1250^\circ\text{C}$ in pure silica glass to $\sim 600^\circ\text{C}$ in soda-lime silicate glass incorporating these two network modifier cations.

Soda can also be dissolved into B_2O_3 , but the initial result is quite different: the glass stiffens and exhibits a minimum in the thermal expansion coefficient around 16mol% Na_2O , exactly the opposite of what happens with soda dissolved into silica. This is known as the “boron anomaly,” an explanation of which is that the addition of Na^+ ions converts vertex-sharing $[\text{BO}_3]$ triangles to vertex-sharing $[\text{BO}_4]$ tetrahedra. On a formally “ionic” model, dissolution of soda into B_2O_3 can be represented as



where ' represents a negative charge, * a positive charge, and \times neutrality with respect to the usual electrostatic expectation at a given site. B^{3+} is in effect oxidized to a B^{4+} valence state, though on a covalent model this is not quite how it happens. Instead, an oxygen ion (electronic configuration: $1s^2 2s^2 2p^6$), introduced to the network and coordinated to a stabilizing near-neighbor Na^+ ion, effectively contributes an electron to a second $2p_y$ orbital in each of two adjacent boron atoms, which in turn hybridize the filled $2s^2$ and resulting half-filled $2p_x^1$ and $2p_y^1$ orbitals into four tetrahedral “sp bonds” extending out to four tetrahedrally coordinating oxygen atoms (each oxygen then has the atom electronic configuration: $1s^2 2s^2 2p_z^2 2p_x^1 2p_y^1$). One mole of Na_2O thus converts four moles of $[\text{BO}_3]$ triangles to $[\text{BO}_4]$ tetrahedra, and a triangular $f = +1$ network into a tetrahedral $f = 0$ network, with a net gain in rigidity. If no other network changes occurred, conversion would be theoretically complete for the composition $0.5\text{Na}_2\text{O}\cdot\text{B}_2\text{O}_3$ —equivalent to composition $\text{Na}_2\text{B}_4\text{O}_7$ (anhydrous borax) which, by analogy to Na-silicate glasses, should comprise a Na^+ -ion-stabilized fully tetrahedral

network). In reality, the $[\text{BO}_4]$ tetrahedral unit occurs in several intermediate configurations based on arrangements of $[\text{BO}_3]$ and $[\text{BO}_4]$ polytopes found in crystalline alkali borate structures⁷—e.g the $[\text{B}_3\text{O}_7]$ triborate and $[\text{B}_5\text{O}_{10}]$ pentaborate units each containing one $[\text{BO}_4]$ tetrahedron per unit, and the $[\text{B}_4\text{O}_{10}]$ diborate unit containing two linked $[\text{BO}_4]$ tetrahedral per unit. The concentration of single $[\text{BO}_4]$ tetrahedra, however accommodated, rises continuously with increasing alkali content up to about 30mol%⁸ and then diminishes as the isolated tetrahedra are replaced in turn by diborate groups and a more extensive tetrahedral network at higher $[\text{BO}_4]$ density.⁹ (It turns out that the anomalous expansion coefficient minimum at 16mol% Na_2O content may arise from an allied but distinguishable phenomenon of phase separation on a nanometer scale into alkali-rich and alkali-poor compositions.¹⁰)

Glass transition

The melting of a glass takes place over a wide range of temperature, corresponding to a gradual loss of viscosity. Like the melting of a crystal at its melting point, the transition from glassy solid to liquid is exothermic and may therefore be monitored by thermal analysis methods. Two common methods of thermal analysis are differential thermal analysis (DTA) and differential scanning calorimetry (DSC); both compare the thermal behavior of a sample to that of an inert reference material. In DTA, both sample and reference are exposed to an identical heat flux during heating or cooling in a furnace; the resulting temperature difference between them is continuously recorded and can be related to changes in the enthalpy or heat capacity of the sample relative to the reference. In DSC, the sample and reference are enclosed in separate furnaces while both are heated; the temperatures of the sample and reference are kept identical by varying the heat delivered to each through changes in the input powers to each furnace, which are continuously compared. The input energy difference (for a chosen small time interval) required to maintain equal temperatures is a measure of the enthalpy or heat capacity change in the sample relative to the reference. The most appropriate thermal analysis method for the relatively low (~ 400 °C) glass transition temperature (T_g) of the alkali borate glasses is DSC.

Because the glass transition is not first order, there is not an *isothermal* enthalpy change as there is for a crystal melting (latent heat of fusion) or crystallization (latent heat of crystallization), so there is usually no distinguishable endothermic peak in the DSC spectrum. Instead, the endothermic *differential* heat flux will at first rise slowly with temperature as the glass network structure begins to change, then rise more quickly as the network structural changes accelerate, then saturate once the sample has terminally liquefied; the inflection point, corresponding to half the heat capacity change, is taken to define the glass transition temperature.

⁷J. Krogh-Moe, *Acta Cryst.* **18** (1965) 77; *Phys. Chem. Glasses* **6** (1965) 46.

⁸P. J. Bray and J. G. O'Keefe, *Phys. Chem. Glasses* **4** (1963) 37.

⁹C. M. Kuppinger and J. E. Shelby, *J. Amer. Ceram. Soc.* **68** (1985) 463.

¹⁰W. Vogel, *Chemistry of Glass* (American Ceramic Society, Columbus, OH, 1985), pp. 101-109.

Sound and Strain

The bonding constraints in a solid act as springs with a characteristic stiffness because the interatomic forces act elastically until the bonds are ruptured. These atomic springs act in concert, so in general the more topologically overconstrained the structure is for a given bond strength, the stiffer the structure. Just as a spring responds to an applied force by extending or contracting, so a solid responds to an applied force by deforming. If the deformation is reversibly proportional to the applied force, the response is termed *linearly elastic*.

1. Linear elasticity.¹¹ Consider a volume element located at some point in the interior of a solid body, with a unit normal \mathbf{n} associated with a unit surface area of the volume element. Suppose force \mathbf{F} , with components F_i along three principal axes ($i = 1,2,3$), acts on this volume element. The force can then be described by the equation

$$\mathbf{F} = \underline{\boldsymbol{\sigma}} \mathbf{n}. \quad (3)$$

The elements of the force \mathbf{F} are

$$F_i = \sum_{j=1}^3 \sigma_{ij} n_j \quad (4)$$

where n_j are the direction cosines (cosines of the angles \mathbf{n} makes with each of the three principal axes) and $\underline{\boldsymbol{\sigma}}$ is what is known as a symmetrical ($\sigma_{ij} = \sigma_{ji}$) second-rank *tensor*, known as the *stress tensor*, with nine elements ($i = 1-3, j = 1-3$). For any surface element, the *normal* stress (force per unit area) is

$$\sigma_n = \sum_{i=1}^3 F_i n_i. \quad (5)$$

The resolved forces F_i cause atom displacements u_j along axes x_j .

Defining $e_{ij} \equiv \partial u_i / \partial x_j$, incremental displacements can be written as

$$du_i = e_{ij} dx_j \quad (6)$$

for small displacements du_i . The e_{ij} comprise the elements of a second-rank asymmetrical tensor $\underline{\mathbf{e}}$, called the *infinitesimal strain tensor*, which is a measure of both rigid body rotation

$$\omega_{ij} = 1/2 (e_{ij} - e_{ji}) \quad (7)$$

¹¹L. W. Hobbs, "Mechanical properties of refractory oxides," in: *Physics and Chemistry of Refractory Oxides*, ed. P. Thévenard (Sitjoff and Noordhof, Leiden, 1982). See also [General Bibliography](#).

and the pure strain (displacement per unit length)

$$\varepsilon_{ij} = 1/2 (e_{ij} + e_{ji}). \quad (8)$$

The strains ε_{ij} comprise the elements of a symmetrical second-rank tensor $\underline{\boldsymbol{\varepsilon}}$, called the strain tensor. If the strain is referred to the principal axes,

$$\underline{\boldsymbol{\varepsilon}} = \begin{vmatrix} \varepsilon_{11} & 0 & 0 \\ 0 & \varepsilon_{22} & 0 \\ 0 & 0 & \varepsilon_{33} \end{vmatrix}; \quad (9)$$

for *uniaxial* strain along axis x_1 , the strain tensor simplifies to $\underline{\boldsymbol{\varepsilon}} = \varepsilon_{11} = e_{11} = \partial u_1 / \partial x_1 \approx u/x_1$ for *small* displacements $u \ll x_1$.

For small strains in a body, the stress at any point is more or less linearly related to the strain, because the interatomic force-separation relationship is sensibly linear. This linear elastic behavior is approximated macroscopically in most solids, though the continuum approach can break down at the atomic level. Linear elastic behavior is just a generalized form of Hooke's law, which can be written

$$\sigma_{ij} = \sum_k \sum_l c_{ijkl} \varepsilon_{kl} \quad (10a)$$

or, more compactly,

$$\underline{\boldsymbol{\sigma}} = \underline{\mathbf{C}} \underline{\boldsymbol{\varepsilon}} \quad (10b)$$

where c_{ijkl} are the elastic *stiffness constants* forming elements of the stiffness matrix $\underline{\mathbf{C}}$. Multiplying (10a) by the reciprocal c_{ijkl}^{-1} produces the equivalent relation

$$\varepsilon_{ij} = \sum_k \sum_l s_{ijkl} \sigma_{kl} \quad (11)$$

where $s_{ijkl} = c_{ijkl}^{-1}$ are called the elastic *compliances*, which comprise the compliance matrix $\underline{\mathbf{S}}$. In their most general forms, $\underline{\mathbf{C}}$ and $\underline{\mathbf{S}}$ contain 81 terms each. Crystal symmetries, reflected in these matrices, dramatically reduce the number of elements; for a *cubic* crystal, for example, the elements are reduced to three constants, c_{11} , c_{12} and c_{44} . For an elastically *isotropic* crystal (properties the same in all directions), only two elastic constants are required, since then

$$c_{44} = 1/2 (c_{11} - c_{12}). \quad (12)$$

The same is true of an isotropic *non-crystalline* material, though the axial labels i,j can no longer be conveniently aligned along convenient crystalline directions, such as unit cell edges; most glasses come under this rubric, since their *average* properties are the same in any direction. This fact enables the behavior of a linearly and isotropically elastic body

to be entirely described by two more recognizable constants, *Young's modulus* Y and *Poisson's ratio* ν , with

$$\begin{aligned} Y &= 1/s_{11} \\ \nu &= -s_{12}/s_{11}. \end{aligned} \tag{13}$$

For a solid defined by orthogonal axes (x_1, x_2, x_3) , Poisson's ratio represents the ratio of *perpendicular* (radial to the axis) to *axial* strains induced,

$$\nu = -\varepsilon_{\perp} / \varepsilon_{\parallel} \tag{14}$$

(*e.g.* stretch a rod and it gets thinner, push on a rubber ball and it gets fatter); it is partially a statement of volume conservation in a material of limited compressibility. Values of Poisson's ratio typically lie between 0.2 and 0.3, although some cellular solids (like cork) can have zero or even negative (!) Poisson's ratios. For a *uniaxially* applied stress σ_1 (where $\sigma_2 = \sigma_3 = 0$) in an isotropic solid, the resulting elastic strains parallel and perpendicular to x_1 are

$$\begin{aligned} \varepsilon_1 &= \sigma_1 / Y \\ \varepsilon_2 &= \varepsilon_3 = -\nu \varepsilon_1 = -\nu \sigma_1 / Y. \end{aligned} \tag{15}$$

Continuum elastic response of solid represents a uniform correlated motion of the constituent atoms (all the atoms respond in the same way: for example, all the atoms move closer together under hydrostatic compression). There are two cases of interest when atoms move less dependently of each other: when a displacement wave passes through the solid (sound, phonon propagation), and when atoms locally perform oscillatory motions with respect to each other in the absence of an external perturbation (*e.g.* thermal vibrations).

2. Sound propagation. Sound is a longitudinal mechanical pressure ($P \equiv$ force/unit area) wave¹² that can be approximated by propagation of a uniaxial stress pulse. For sound propagation in an (isotropic) liquid, necessarily contained by walls, the relevant materials properties are the compressibility

$$\kappa = -\rho \partial P / \partial \rho \tag{20}$$

[or its reciprocal, the bulk modulus $B \equiv 1/\kappa = -(1/\rho) \partial \rho / \partial P$] and density. The sound propagation velocity is given by

$$v_s = \sqrt{B/\rho}. \tag{21}$$

¹²Allan D. Pierce, *Acoustics: An Introduction to its Principles and Applications* (Optical Society of America, Melville, NY, 2005)

For an isotropic solid, where expansion or compression can take place perpendicular to the propagation axis through the Poisson effect, the relevant materials are analogously Young's modulus and density, and the propagation velocity of an acoustical pulse is given by

$$v_s = \sqrt{Y/\rho}. \quad (22)$$

Since typical mechanical moduli for strongly-bonded solids (metals, ceramics) are in the 50 GPa range with densities $\sim 1-10 \times 10^3 \text{ kg/m}^3$, sound velocities in these solids are of order $v_s \sim 5000 \text{ m/s}$. Measurement of the speed of sound in a solid thus provides another convenient way to obtain its Young's modulus.

3. Normal Modes of Vibrations in Solids. In order to understand other vibrations of atoms with respect to each other in solids, it is instructive to consider vibrations in simpler model systems such as a series of masses held together with springs. The concept of *normal modes* has central importance in the analysis of such systems.. Normal modes: are the vibrational modes that decouple the energy problem, *i.e.* they diagonalize the Hamiltonian of the system. As a simple example, consider a system of three identical masses m kept together by four spring of constant g , as shown in Fig. 1. In order to solve the classical problem of the oscillations of these masses the first thing to do is to set a system of coordinates that conveniently describes the system. In this particular case, we will assume that the masses can move only along the mass-mass direction, that is we will consider only the one dimensional problem. As shown in Fig. 1, the first choice that we can make is to assign a series of internal coordinates x_i that describes the displacement of masses from their rest positions.

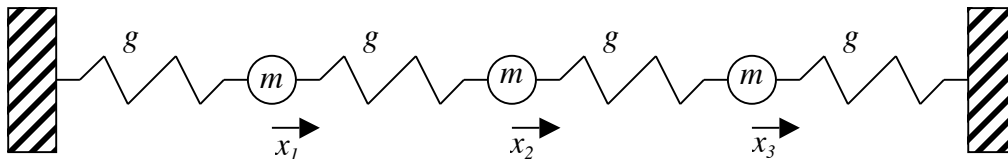


Figure 1. Schematic drawing of a series of equal masses held together by equal massless springs. The boxes at the extremes represent unmovable infinite masses.

Classically this system can be solved by first writing its Hamiltonian in function of the three internal coordinates (x_1, x_2, x_3) and of the three momenta of the particles ($p_1, p_2,$

$$H \equiv T + V \equiv \frac{p_1^2}{2m} + \frac{p_2^2}{2m} + \frac{p_3^2}{2m} + \frac{1}{2}kx_1^2 + \frac{1}{2}k(x_2 - x_1)^2 + \frac{1}{2}k(x_3 - x_2)^2 + \frac{1}{2}kx_3^2 \quad (23)$$

where T and V are the total kinetic and potential energy of the system. A complete solution of the system is then determined by solving the six differential equations

$$\begin{cases} \frac{\partial H}{\partial p_i} = \frac{dx_i}{dt} \\ \frac{\partial H}{\partial x_i} = -\frac{dp_i}{dt} \end{cases} \text{ with } i = 1, 2, \text{ and } 3 \quad (24)$$

It should be evident that all of these equations will depend on at least *four* of the system variables.

It can be shown that there always exists a linear combination of the internal coordinates, called normal coordinates, that generates a Hamiltonian that is simply the sum of the three independent Hamiltonians. A consequence of this is that the solution of the vibrational problem of the system becomes the solution of three simpler and independent problems. Each solution is a normal mode of vibration, that is, a vibration that happens at a given energy. In this particular problem, by introducing the following variables

$$\begin{cases} X = x_1 - x_3 \\ Y = x_1 - \sqrt{2} x_2 + x_3 \\ Z = x_1 + \sqrt{2} x_2 + x_3 \\ P_1 = p_1 - p_3 \\ P_2 = p_1 - \sqrt{2} p_2 + p_3 \\ P_3 = p_1 + \sqrt{2} p_2 + p_3 \end{cases} \quad (25)$$

it can be shown that the Hamiltonian becomes

$$\begin{aligned} H &= \frac{P_x^2}{2m} + \frac{P_y^2}{2m} + \frac{P_z^2}{2m} + \frac{1}{2}kX^2 + \frac{1}{2}kY^2 + \frac{1}{2}kZ^2 = \\ &= \left(\frac{P_x^2}{2m} + \frac{1}{2}kX^2 \right) + \left(\frac{P_y^2}{2m} + \frac{1}{2}kY^2 \right) + \left(\frac{P_z^2}{2m} + \frac{1}{2}kZ^2 \right) = H_x + H_y + H_z \end{aligned} \quad (26)$$

Each Hamiltonian can be solved independently and indeed the whole system can be solved by solving the three independent systems

$$\begin{cases} \frac{\partial H}{\partial p_x} = \frac{dX}{dt} \\ \frac{\partial H}{\partial X} = -\frac{dp_x}{dt} \end{cases} \quad \begin{cases} \frac{\partial H}{\partial p_y} = \frac{dY}{dt} \\ \frac{\partial H}{\partial Y} = -\frac{dp_y}{dt} \end{cases} \quad \begin{cases} \frac{\partial H}{\partial p_z} = \frac{dZ}{dt} \\ \frac{\partial H}{\partial Z} = -\frac{dp_z}{dt} \end{cases} \quad (27)$$

Each system has as a solution a simple harmonic wave equation of the type

$$X = C \exp(i\omega t) \quad (28)$$

where C is a real number that specifies the vibrational amplitude of the normal mode and ω is the frequency of oscillation of the normal mode. We recall that the normal modes are those particular vibrational modes of a system that decouple the energy problem, that is, they allow the separation of the Hamiltonian into independent Hamiltonians. (This property in linear algebra is called orthogonality.) Additionally, it can be shown that any system vibration is always a linear combination of normal modes.

This classical derivation of the normal modes can be extended trivially in quantum mechanics simply by replacing the classical energy expression with the quantum mechanical operators. Even in that case, it can be shown that the normal modes are the ones that allow for the separation of the Hamiltonian of the system into independent Hamiltonians. In quantum mechanics, we know that frequency and energy are related by the relation

$$U = h\nu = hc/\lambda = hc\omega \quad (29)$$

where ν is the frequency (expressed in s^{-1}), while $\omega = 1/\lambda$ is the wavenumber (generally—but not following SI convention—expressed in cm^{-1}), h is Planck's constant ($6.626 \times 10^{-34} \text{ J s}$) and c is the speed of light in vacuum ($2.99792458 \times 10^{10} \text{ cm/s}$). Thus, each normal mode has its own energy.

4. Molecular Dynamics. A molecule can be seen as an isolated system of atoms (masses) held together by forces around their equilibrium position. Let's first look at a diatomic molecule. The energy that keeps the molecule together is shaped as illustrated in Fig. 2. Around the equilibrium position, the energy increases as the square of the displacement; that is, the energy is that of a spring (or of a systems of springs) that holds the atom in place. As demonstrated in 3.012, a particle in such a parabolic potential (a linear harmonic oscillator) has quantized energy levels that are evenly spaced. These energy levels are the vibrational levels of the molecule. Their frequency of oscillation is determined by the difference in energy ΔU between the vibrational states

$$\nu = \Delta U / h = (1/2\pi) \sqrt{k/\mu}, \quad (30)$$

where k is the spring constant and $\mu = m_1 m_2 / (m_1 + m_2)$ is the reduced mass.

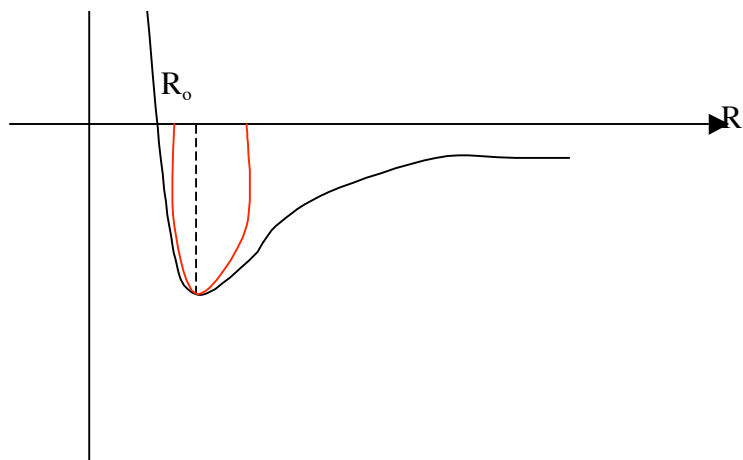


Figure 2. Schematic drawing of an energy-position plot for a diatom molecule. R represents the distance between the atoms. As shown from the red line near the equilibrium position (R_0) the energy barrier can always be approximated by a parabola and thus the bond can be treated like a spring.

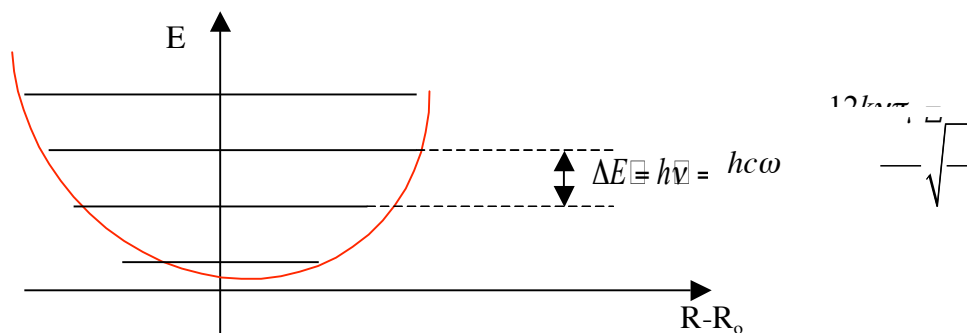


Figure 3. Distribution of the vibrational energy levels in a linear harmonic oscillator. ν is the frequency expressed in s^{-1} , while ω is the wavenumber expressed in cm^{-1} .

The vibration frequencies for some simple diatomic molecules (Table 1) are seen to fall in the infrared region of the electromagnetic spectrum.

Table 1. Stretching Frequencies for some Diatomic Molecules

Molecule	μ (amu)	k (pN/nm)	ω (cm^{-1})
H_2	0.5	0.52	4160
D_2	1.0	0.52	2940
HF	0.95	0.88	3950
HCl	0.97	0.48	2885
HBr	1.00	0.39	2559
HI	1.00	0.29	2230

A polyatomic molecule composed of N atoms has $3N$ degrees of freedom, of which 6 (5 in the case of linear molecules) are the 3 translations and the 3 rotations of the molecule

as a whole and thus do not change the relative distances between molecules. The other $3N-6$ are vibrational degrees of freedom of the molecules. For each degree of freedom there is a normal mode of vibration. While the energy-position plot of for a diatomic molecule is a two-dimensional plot, the same plot for a polyatomic molecule becomes a $(3N-6)+1$ dimensional surface of a very complex shape. If this surface is sectioned by a plane that follows the displacement along a normal mode then (at least around the equilibrium position) the plot will look exactly like the one in Fig. 2. This is the beauty of normal mode formalism.

Some normal modes are localized mostly on a few atoms and consequently are used to detect the configuration of those atoms, while others are distributed along the whole molecule and thus can be used to extract information about the whole molecule. An example of the former is the “breathing mode” of a connected group of atoms, such as the $[B_3O_6]$ boroxyl ring. This mode is modified in frequency by substitution of the tetrahedral $[BO_4]$ units for one (or more) of the $[BO_3]$ triangles in the boroxyl ring.. Examples of the latter are bending modes of pieces of the borate network as it is increasingly broken up by Na additions, for example the B-O-B bending mode. Both are discussed below.

Vibrational Mode Spectroscopy

Light passing through or reflected from solids can interact with the constituent atoms or molecules. Familiar examples are the opacity of metals and semiconductors, the cobalt-blue color of glasses containing cobalt ions, and the stopping of the sun’s ultraviolet radiation by spectacles or window glass. These examples each arise from *absorption* of light photons that contribute *all* of their quantum energy to exciting electrons of the atom or solid to available higher electronic states (and are therefore lost and disappear). Absorption of infrared light photons similarly occurs by exciting mechanical vibrations (at $\sim 10^{13}$ Hz frequencies) of atoms, groups of atoms, or molecules in a solid.

Chandrasekhara Raman (1888-1970), an Indian physicist, noted in 1928 that a very small portion of light passing through matter (about 1 in 10^7 photons) is scattered with a small change in wavelength; the analogous phenomenon was known already for X-rays (Compton scattering,¹³ discovered by American physicist Arthur H. Compton (1892-1962) in 1923, for which he shared the Nobel Prize in physics for 1927) but was unexpected for light. Raman (by virtue of communicating news of his discovery to the journal *Nature*¹⁴ by cable rather than by mail, ahead of two Russian competitors who made the discovery 5 days later but posted their paper to the journal *Naturwissenschaften*) was first to report this discovery, for which he shared the Nobel Prize in physics for 1930 (with C. T. R. Wilson, inventor of the cloud chamber) and was also knighted.

¹³A. H. Compton, “Absorption Measurements of the Change of Wavelength Accompanying the Scattering of X-Rays, *Philos. Mag.* **46**[275] (1923), 897-911; “The Spectrum of Scattered X-Rays,” *Phys. Rev.* **22**[5] (1923) 409-13.

¹⁴C. V. Raman and K. S. Krishnan, “A new type of secondary radiation,” *Nature*, **121**[3048] (31 March 1928) 501; C. V. Raman, “A new radiation”, *Indian J. Phys.* **2** (1928) 387.

Both infrared absorption and the Raman effect involve electronic states of a molecule or groups of atoms in a solid that are coupled to vibrational modes of the entity (generating so-called “*vibronic*” states). In infrared absorption, a light photon of specific wavelength λ (and corresponding quantum energy $U = hc/\lambda$) effects an energy transition from the zeroth-order vibrational level of the ground electronic state to the first excited vibrational level of the ground electronic state, provided there is a change in the molecular dipole during the vibration. For example, the dipole moment does not change in stretching a chlorine molecule (Cl_2), so that normal mode is not observable in the IR absorption spectrum (IR-active mode), whereas stretching an acid chloride (HCl) does change the dipole moment and leads to an IR-active mode.

In Raman scattering, the electromagnetic field of a light photon of *higher energy* (say, in the visible, not the IR) interacts as well with the entity’s electrical polarizability, inducing a *more energetic* transition from (say) the zeroth-order vibrational level of the ground electronic state to some other vibrational level of a higher electronic state. The polarizability is the ability of a molecule or group of atoms to form a dipole in the presence of an electromagnetic field, which in the above example can lead to a dipole moment for Cl_2 stretching and a Raman-active mode. That excitation is followed by prompt re-emission of a second photon (in $\sim 10^{-14}$ s) consequent upon de-excitation of this excited vibronic state to (say) the first excited vibrational level of the ground electronic state (*Rayleigh scattering*). The difference in energy between the incoming photon—which is lost to exciting the initial vibronic excitation—and the re-emitted photon is thus just the energy difference between the zeroth-order and first-order vibrational states of the electronic ground state, *viz* the transition energy observed for the specific infrared absorption. It appears to the observer, therefore, that the incident photon has been scattered with a discrete energy loss, corresponding to this infra-red transition, and the scattered photons thus appear shifted to the red by the energy of this vibrational transition; this shift is called the Raman shift, traditionally measured in wavenumbers ($1/\lambda$ in cm^{-1} , proportional to transition energy).

The absorption, excitation and decay processes for a Raman process are diagrammed in Fig. 4. An electromagnetic radiation quantum (photon) of energy much higher in energy than that of the vibrational excitation quantum is sent to the sample. A transition is made in the sample from an initial vibrational state in the ground electronic state to an excited electronic state, from which it immediately decays back. In most cases, the system returns to its original vibronic state, emitting another photon of the same energy (normal Rayleigh scattering). But in rare cases the system will decay vibronically to a *different* final vibrational state, emitting a photon different in energy from the incident photon by an amount equal to difference between the initial and final *vibrational* state energies. When the system starts in lower vibrational state and decays from the excited vibronic state to a higher final vibrational state, the event is known as Stokes scattering; when the systems starts from a higher vibrational state and decays to a lower final vibrational state, the event is known as anti-Stokes scattering. An interesting feature of Raman spectroscopy is that the intensity difference between the Stokes and the anti-Stokes lines depends only on the temperature, and thus Raman spectrometers can be used as non-invasive thermometers.

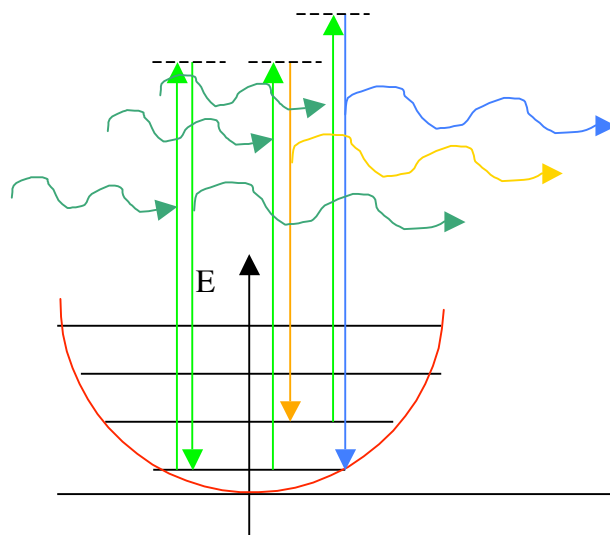


Figure 4. Schematic drawing of the three possible off-resonance interactions between an electromagnetic wave and a molecule. In the case of Rayleigh scattering a photon gets absorbed and immediately reemitted without gaining or losing energy (left). In the case of anti-Stokes scattering, a photon excites a particle that is in the first vibrational state. The particles then decays in the second vibrational state, losing energy (right). The opposite happens in Stokes scattering. (middle)

In borates glasses, two sharp Raman peaks of interest have their origin in the “breathing” vibrational mode of $[\text{B}_3\text{O}_6]$ boroxyl rings containing only $[\text{BO}_3]$ triangle subunits ($\sim 805 \text{ cm}^{-1}$ peak) and boroxyl rings in which a $[\text{BO}_4]$ tetrahedron has replaced one of the $[\text{BO}_3]$ triangles in the ring (so-called “triborate group”, $\sim 775 \text{ cm}^{-1}$ peak).¹⁵ The relative populations of these two peaks change with increasing alkali ion additions as $[\text{BO}_4]$ units are increasingly created.¹⁵⁻¹⁷ For example, if all boron atoms were accommodated in $[\text{BO}_3]$ or $[\text{BO}_4]$ units arranged only in $[\text{B}_3\text{O}_6]$ boroxyl rings and $[\text{B}_3\text{O}_7]$ triborate groups in a fully connected network (no non-bonded oxygens), then the fraction of boroxyl groups remaining is given¹⁵ by $(2 - 8M)/3$; this fraction would be 27% for $M = 15\text{mol}\% \text{ Na}_2\text{O}$ and 13% for $M = 20\text{mol}\% \text{ Na}_2\text{O}$. Another characteristic peak at 450 cm^{-1} corresponds to symmetrical stretching of the two bonds to a bridging oxygen (in the B-O-B link). Other vibrational modes appearing in the Raman spectra additionally occur as the B_2O_3 network is broken up by formation of non-bonded oxygens with the addition of alkali ions.¹⁸ The most prominent, between 1200 and 1500 cm^{-1} , are assigned to

¹⁵T. W. Brill, “Raman spectroscopy of crystalline and vitreous borates,” Dr. Tech. Wetenschappen thesis, (T. H. Eindhoven, 1976) 127pp.

¹⁶W. L. Konijnendijk and J. M. Stevels, “The structure of borate glasses studied by Raman scattering,” *J. Non-Cryst. Solids* **18** (1975) 307-31; W. L. Konijnendijk, *Philips Res. Repts.*, Suppl. No. 1 (1975).

¹⁷R. E. Youngman and J. W. Zwanziger, “Network modification in potassium borate glasses: Structural studies with NMR and Raman spectroscopy,” *J. Phys. Chem.* **100** (1996) 16720-28.

¹⁸T. Yano, N. Kunimine, S. Shibata and M. Yamane, “Structural investigation of sodium borate glasses and melts by Raman spectroscopy: I. Qualitative evaluation of structural units,” *J. Non-Cryst. Solids* **32**[3] (2003) 137-146; II. Conversion between $[\text{BO}_4]$ and $[\text{BO}_2\text{O}^-]$ units at high temperature,” *ibid.* 147-56.

various vibrational modes of increasingly *isolated* [BO₃] units in an increasingly disconnected network.

Experimental Procedure

1. Glass melting. In this experiment, you will melt a series of alkali borate glasses with compositions 10, 15, 20, 23, 25, 28.5, 30, 40 and 45 mol% Na₂O. These will have been produced by reacting sodium carbonate (Na₂CO₃) with boric acid (H₃BO₃). Because the Na and B come from different reactants that are measured out separately by weight, it is common to represent the glass composition as RNa₂O•B₂O₃, instead of by the alkali mole fraction M (*i.e.* as MNa₂O•[1-M]B₂O₃), where the relative constituent oxide ratio R = M/(1-M) or M = R/(1+R). The stated mole fractions therefore correspond to R = 0.091, 0.176, 0.25, 0.30, 0.33, 0.40, 0.43, 0.67 and 0.82. The two starting ingredients decompose on heating and reacting



Accompanied by evolution of large volumes of (volatilized) gas that can lead to considerable foaming of the product until fully evolved. For this reason, the constituents are heated together slowly in a box furnace, beginning at 200 °C and increasing temperature by 100 °C increments every 30 minutes to 1000 °C. Because of time constraints, glasses of these compositions have been prepared in advance in 250 ml alumina crucibles, poured into smaller 50 ml alumina crucibles for ease of handling, and cooled. Nevertheless, as an exercise you should calculate the weights of each constituent required to produce the 50g or so of final product glass for each composition.

2. Glass fiber drawing and the glass transition. Reheat the crucibles and glass contents to 900 °C in a box furnace to remelt the glasses. The furnace containing the R = 0.82 sample may need to be heated to 950 °C in order to melt the solid. Each melted product should, at 900-950 °C, be a low viscosity clear liquid without bubbles. Withdraw each crucible in turn with tongs and set it on an insulating brick. While one group member holds the hot crucible with tongs, another should take a ~200 mm length of 4-mm diameter vitreous silica rod and dip one end of the rod into the glass melt, withdrawing the rod *slowly* so as to draw out a glass rod or fiber at least 2-mm in diameter and 100 mm in length if possible. The drawing operation needs to be carried out slowly and at a critical viscosity (similar to that of honey or molasses), achieved over a small temperature range somewhat above T_g, as the glass in the crucible cools. Drawing will stop rather suddenly when the melt cools significantly below this temperature range. Using diagonal cutters, cut the fiber near to the now-solidified melt surface and, when cool, break it off from the silica rod. You will want to draw at least one fiber of each composition and will need to reheat the crucible to 900 °C for 15 minutes between drawings if you need to draw again. Keep fibers of different compositions separate in labeled trays or envelopes. Make note of your qualitative impression of the comparative viscosities of each melt when first extracted from the

furnace at 900-950 °C and the comparative times taken for the crucibles to cool to where the viscosity is suitable for fiber drawing. Comment on any anomalous result and explain its significance.

3. Measurement of glass transition temperature by DSC. Break and small piece off the end of the fiber drawn from one glass composition, crush, and place in the aluminum specimen pan of a differential scanning calorimeter (DSC) instrument and cap the pan. Prepare a second capped pan which is empty. Ramp up the temperature using the recommended heating rate protocols and determine the glass transition temperature T_g for this glass composition from the shape of the differential endotherm curve. The maximum temperature is limited by the melting point ($T_m = 660$ °C) of the aluminum pans.

4. Raman spectroscopy measurements. The apparatus used is a confocal Raman microprobe, which provides a highly focused spot of laser light on the sample, with the scattered light being collected through the same optics into an optical fiber and sent into a grating spectrometer. Raman microprobe measurements can easily be carried out in reflection, as well as transmission, either on small pieces of the drawn glass fibers or even more conveniently on the surface of the solidified glass at the bottom of the crucibles. In this experiment, laser photons with 745 nm (red, 1.66 eV) wavelength are used for excitation. The Raman shift will be measured from about 100 to 2000 cm^{-1} (this corresponds to the Raman-scattered photons being shifted to longer wavelengths (lower energies) by between +6 nm (-0.012 eV) and +878 nm (-0.25 eV). Measure the Raman spectrum for each of the glass compositions being investigated and note the evolution of the principal Raman peaks with glass composition. Relate the associated network entities responsible for these peaks to the evolution of the sodium borate glass network structure.

General Bibliography

Robert H. Doremus, *Glass Science* [2nd ed.] (Wiley, New York, 1994).

E. J. Hearn, *Mechanics of Materials* [3rd edition], Volume 1: *An Introduction to the Mechanics of Elastic and Plastic Deformation of Solids and Structural Materials* (Elsevier, New York, 1997).

W. David Kingery, H. K. Bowen and Donald R. Uhlman, *Introduction to Ceramics* [2nd ed.] (Wiley, New York, 1976).

A. E. H. Love, *A Treatise on the Mathematical Theory of Elasticity* [4th edition] (Dover, New York, 1944).

W. B. Person and G. Zerbi, eds., *Vibrational Intensities in Infrared and Raman Spectroscopy* (Elsevier Scientific Publishers, Amsterdam, 1982).

James E. Shelby, *Introduction to Glass Science* (Royal Society of Chemistry, London, 1993).

Catherine J. Simmons and Osama H. El-Bayoumi, *Experimental Techniques of Glass Science* (The American Ceramic Society, Westerville, OH, 1993).

Arun K. Varshneya, *Fundamentals of Inorganic Glasses* (Academic Press, New York, 1994).

W. Vogel, *Chemistry of Glass* (The American Ceramic Society, Columbus, OH, 1985).